

OPTIMIZATION AND DESIGN OF THE AIR CORE COMPULSATOR FOR THE CANNON CALIBER ELECTROMAGNETIC LAUNCHER SYSTEM (CCEML)

By:

S.B. Pratap
J.R. Kitzmiller
T.A. Aanstoos
K.G. Cook
R.N. Headifen
R.A. Kuenast
R.A. Lee
H-P Liu
D.J. Wehrlen

Digest of Technical Papers of the 9th IEEE International Pulsed Power Conference,
June 1993, vol. 1, p. 29

PN - 213

Center for Electromechanics
The University of Texas at Austin
PRC, Mail Code R7000
Austin, TX 78712
(512) 471-4496

OPTIMIZATION AND DESIGN OF THE AIR CORE COMPULSATOR FOR THE CANNON CALIBER ELECTROMAGNETIC LAUNCHER SYSTEM (CCEML)

S.B. Pratap, J.R. Kitzmiller, T.A. Aanstoos, K.G. Cook, R.N. Headifen,
R.A. Kuenast, R.A. Lee, H-P Liu, and D.J. Wehrlein

Center for Electromechanics
The University of Texas at Austin
BRC, Mail Code 77000
Austin, TX 78712

Abstract

The Center for Electromechanics at The University of Texas at Austin (CEM-UT) is currently in the manufacturing phase of a skid mounted, compulsator driven 30 mm (round-bore equivalent), rapid fire railgun system. The objective of the 30-month program is to develop a compact, lightweight test bed capable of launching three, five-round salvos of 185-g payloads to 1.85 km/s at a firing rate of 5 Hz. Per contractual requirement, the system is also fully compatible with the Amphibious Assault Vehicle (AAV). This paper describes the results of the optimization process used in determining the power supply requirements for the CCEML. The paper presents the performance specifications and design of the compulsator and critical power electronics resulting from the optimization process. The compulsator (CPA) is a four-pole, self-excited, air-core design which stores the energy for all three salvos inertially.

Introduction

The team of (prime contractor) FMC-NSD and (sub-contractors) CEM-UT and KAMAN Sciences Corporation (KSC) are currently in the design phase of a 30 month effort to design, build, and test an electromagnetic (EM) launcher technology demonstrator with program goals as summarized in table 1. A unique aspect of the program requirements was that desired subprojectile performance at the target was specified; no specifics relative to EM power supplies or system configurations were given. Determining the optimum system configuration required an intensive tradeoff study which looked at nearly all facets of the current EM state-of-the-art including battery-inductor pulsed forming networks (PFN), flywheel-alternator-capacitor PFNs, homopolar generator-inductor PFNs and compulsator PFNs. The results of the tradeoff analysis showed a four-pole, self-excited, field regenerative, selective passive air-core compulsator (CPA) design to be the best choice to satisfy contractual requirements.

Following the tradeoff analysis, the four-pole CPA design was optimized around five independent parameters including launch package mass, muzzle velocity, pulse width, number of shots stored inertially in the rotor, and number of salvos stored inertially in the rotor. In all, over 400 cases were analyzed, each producing a specific optimum CPA design. The overall system optimum configuration settled on launching 15, 185 g launch packages (95 g sub projectile mass) in three, five-shot salvos with a muzzle velocity of 1850 m/s. The shot rate is 300 cpm with a 2.5 s dwell between salvos.

The first part of this paper describes the CPA optimization process and results, as well as predicted performance of the

Table 1. CCEML SOW requirements

| | |
|---|---|
| Armor Penetration (0° and (56°) obliquity] | 73 mm (131mm) RHA @ 1,500 m 37 mm (66mm) RHA @ 3,000 m |
| Caliber | 20 -40 mm |
| Firing Rate | 300 - 400 rnds per minute |
| Salvo Size | 5 to 7 rounds (3 salvos total) |
| Time Between Salvos | 2-2.5 s |
| Probability of Hit | 0.9 |
| System Weight | 5,000 lb maximum |
| Weapon Mounting Platform | compatible with AAV |

compulsator. In the second part, the CPA mechanical design is presented, including operating characteristics, general specifications, and design and operation of the power electronics.

CPA Performance and Optimization

The unique aspect of the specifications in this system was that instead of constraining the muzzle energy in the launch package, the penetration at the target at 1.5 and 3.0 km was constrained. This allowed the team to look at some broader, system wide tradeoffs since the launch package mass and the velocity at the muzzle were flexible parameters. Referring back to table 1, the system optimization considered specific issues such as dispersion at the muzzle and the probability of hit in order to determine the optimal shots per salvo and salvos per mission.

In the optimization process the starting point was the design of the penetrator rod (sub-projectile) which was performed by KSC. This was a logical starting point since each sub-projectile was required to meet the penetration requirements at the target. Three different penetrator nose tip radii were considered for five muzzle velocities. The velocity ranged from 1.7 km/s to 2.3 km/s in increments of 150 m/s. For each velocity/nose tip, a projectile was designed with the appropriate aeroballistic and penetration characteristics. Three pulse widths (1.4, 1.7, and 2.0 ms) with the same acceleration ratio (0.5) were considered, implying three peak accelerations which were considered. It was determined that the mid-drive penetrator was not significantly different for the three peak acceleration designs. However the mid-riding tandem solid armature was affected by the peak acceleration issues. This resulted in a total of 45 different launch package designs with corresponding muzzle kinetic energy requirements.

For each of these launch packages an optimized launcher was designed. In this case, optimum was defined as a barrel/launch package combination that resulted in a minimum breech energy requirement. Several interesting tradeoffs were developed as the result of the study.

Augmented vs. Simple Railgun

As indicated earlier the uniqueness of this system was that target penetration requirements rather than muzzle energy was specified. This truly presented an opportunity to minimize the muzzle energy. In any EM launcher the useful energy is that which is imparted to the subprojectile. All other energy including the kinetic energy in the armature represents a loss. An augmented gun typically has extra losses associated with the augmenting turn, with the result that if the muzzle energy of the launch package was fixed it would indicate a higher breech energy requirement. However, with an augmented gun the action ($\int i^2 dt$) through the armature is lower with the result that the armature can be lighter thus resulting in lower muzzle energy requirements. It is therefore conceivable that the breech energy requirements in the augmented gun be lower than a simple gun. Indeed, this was our observation on the CCEML system which finally led to the selection of the augmented gun.

Energy Storage

The pulsed power and energy storage system selected for the CCEML was the compulsator. The size and weight of the pulsed power supply was driven to a large extent by the manner in which energy was apportioned between the prime power and the pulsed power. Considering that the time between salvos is only 0.2 s for a 300 cpm firing rate it is evident that enough kinetic energy needs to be stored in the rotor to complete one salvo. The time between salvos is 2 to 2.5 s. Recharging between salvos requires lower power than recharging between shots but is still considerably high, requiring a turbine which is less traceable to the AAV. However, to conduct an effective tradeoff study machines were designed to store one, two, and three salvos with five, six, and seven shots per salvo, i.e. a total of nine machines for each barrel/launch package combination. The total number of machines thus designed was $45 \times 9 = 405$. Figure 1 summarizes the results of the optimization process. The machine mass was most sensitive to the energy stored in the rotor. Typically it showed a lower mass increment for higher energy storage. This is because given a pulse width, the rotational speed is fixed. Higher energy storage is obtained with larger machine radii and therefore higher energy densities. Over the range of parameters considered the sensitivity of the machine mass to projectile velocity, pulse width and nose tip radius was not significant. For a given energy storage the various machines fell within a 100-g window.

Probability of hit analyses performed by FMC-NSD required a total of three salvos and five shots per salvo at 300 rpm. Considering integration issues it was decided that the machine store enough energy to complete all 15 shots without re-motoring.

Pulse Shape

Three pulse shapes were considered (fig. 2). The common feature in these pulse shapes is that each one has the same peak

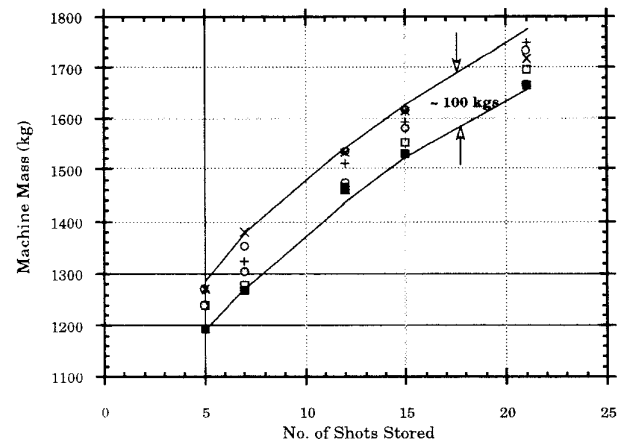


Figure 1. Summary of machines investigated

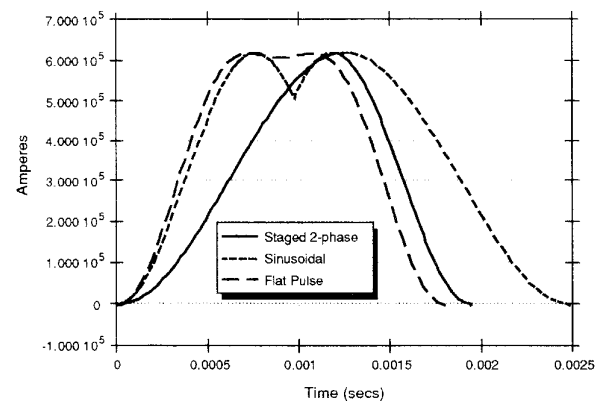


Figure 2. Comparison of various pulse shapes

current and each have the same action. These pulse shapes were obtained with the passive, selective passive, and the staged discharge machines. The acceleration ratio with the passive machine is about 0.38 and the other machines have a ratio of between 0.5 and 0.6. The staged discharge machine is at present an unproved concept and to minimize risk on this project was not pursued. Of the other two pulse shapes, the selective passive machine has a better acceleration ratio and also has a shorter pulse width. This indicates that the machine can spin faster and has a higher energy density. Thus there is a correlation between the pulse shape and the energy density which resulted in the selection of the selective passive machine.

Number of Poles

To get the longest pulse width at the highest tip speed, and therefore highest energy density, it was necessary to keep the number of poles to a minimum. This was especially true of the single phase variant of the compulsator. When energy limited systems are being considered energy density needs to be maximized which normally results in the selection of a two pole machine. However there are some difficulties with a two-pole design. The shaft of the rotor would have to spin through a high magnetic field with a two-pole design. Using a conductive shaft material causes

severe eddy currents. This results in two options, neither of which are desirable. One is to use a ceramic shaft and the other is to use a copper clad metallic shaft. In the latter option the copper which acts as a shield would have to be actively cooled.

The force distribution in a two pole machine is quite non-uniform during discharge. The center of force on the two-pole windings is at diametrically opposite points. This results in higher stresses. The non-uniformity of pressure results in local bending which adds to the hoop stress in the rotor. Also, it is difficult to manage the deflections under the non-uniform loading especially when the clearances between stationary and rotating parts need to be at a minimum.

With the four-pole machine, the field strength reduces at distances away from the field winding towards the center, until at the center the field strength is zero. This permits the use of a conductive shaft which suffers much lower eddy current losses. Also the four-pole winding has the center of force distributed at four equidistant points along the circumference. This load distribution is much easier to manage. Considering these and other advantages the four-pole geometry was selected.

Performance of the System

In a typical operating mode the machine will be driven by a slip clutched, frequency controlled 400 hp (peak) induction motor to a top speed of 12,000 rpm. The torque speed curve will be actively controlled to enable the machine to optimally negotiate the first critical speed. After reaching the top speed the discharge sequence will commence. A typical shot has three distinct events. In the first 100 ms the field coil is charged in a self excitation mode. To initiate this process a capacitor is first discharged into the field coil which provides the seed current. At full field, main gun discharge takes place over 2 ms. Over the next 90 ms part of the magnetic energy stored in the field coil is recovered and returned to the rotor. Throughout the field charging process the motor drives the rotor. During the main discharge when the torque exceeds 400 ft-lb the clutch connecting the motor to the rotor of the compulsator slips thus isolating the motor from the high decelerating torque. After the discharge is complete the motor resynchronizes with the rotor in about 15 ms. In this manner energy is being delivered to the rotor at a slow rate throughout the mission.

The peak current in the gun ranges from 790 kA for the first shot to 650 kA in the last shot. The launch package muzzle energy remains the same for all shots. Figure 3 shows the 15 current pulses during a full engagement. Figure 4 shows variation in the machine speed over the engagement. A little over 50% of the energy is used during a full engagement. The majority of the shots take place without a muzzle arc. However since the machine does slow down to about 70% of its original speed over a full engagement, the last few shots need a muzzle switch to suppress the muzzle arc and ensure that the projectile has minimal dispersion at exit.

CPA Design

CPA Topography and Specifications

As outlined above, the CPA is a four-pole, air-core, selective-passive design which is self-excited and regenerates field energy

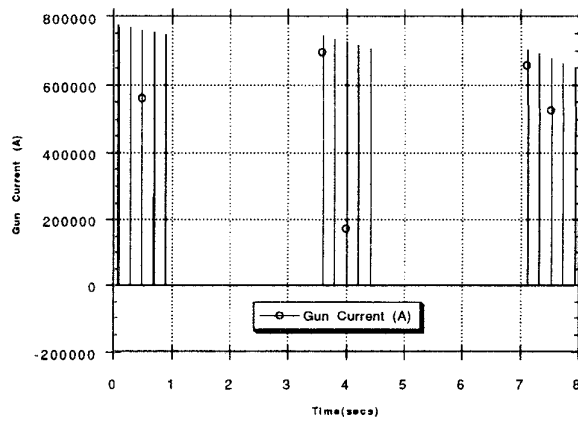


Figure 3. CCEML gun current and machine current during a mission

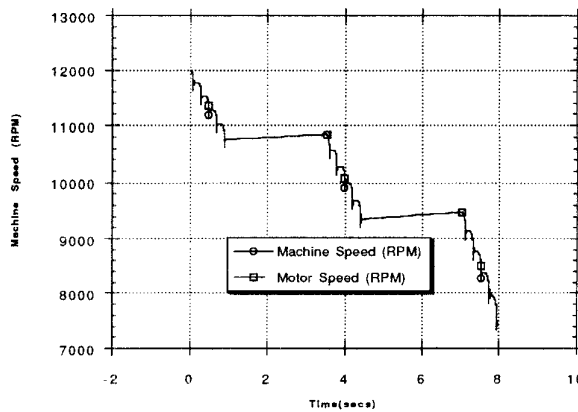


Figure 4. CCEML machine and motor speed during a mission

between each shot. Table 2 lists the CPA pertinent operating specifications. Figure 5 shows the longitudinal cross section of the compulsator. This generation of CPA utilizes a combination of the most attractive features found in previous designs including the Task-C range gun and Small Caliber Compulsator systems [1,2,3]. As discussed above, the four pole design allows for the use of a monolithic through shaft, which is Ti 6Al-4V for the CCEML generator. The CCEML generator features an all titanium stator structure which is made up of four custom castings. The composite rotor is supported on hybrid rolling element bearings which are suspended in full hydrostatic bearing dampers to control dynamic response. Great emphasis was placed on minimizing the CPA weight which makes up for about 70% of the entire system weight.

In the following sections more detail is presented for specific critical components making up the CPA. Also included is a section on the design and operation of the CPA's power electronics.

Rotor

Energy storage for the Cannon Caliber compulsator power supply is provided by a composite flywheel, four pole rotor armature winding, and hoop wound composite banding, all supported on a titanium shaft. The rotor winding serves both excitation and armature duty by means of an external rectifier/inverter discussed

Table 2. CCEML CPA performance parameters

| | | |
|-------------------------------------|--------|-------------------|
| Design Speed | 12,000 | rpm |
| Energy Storage | 40 | MJ |
| Peak Field | 2 | T |
| Peak Open Current Voltage | 3.84 | kV |
| Peak Design Current | 800 | kA |
| Peak Power | 2.4 | GW |
| Discharge Torque | 2.0 | MN-m |
| Electrical Frequency | 400 | Hz |
| Pulse Width | 2 | ms |
| Action (Full Engagement) | 9.15 | GA ^{2-s} |
| Stored Energy Density | 19.3 | J/g |
| Specific Energy Density | 47.6 | MJ/m ³ |
| Power Density | 1160 | W/g |
| Delivered Energy Dens. (Shot) | .29 | J/g |
| Delivered Energy Dens. (Engagement) | 4.35 | J/g |

later in this paper. The rotor assembly has the following specifications:

- diameter 28.66 in. (0.73 m)
- rotor length 39.28 in. (1.00 m)
- overall shaft length 70.78 in. (1.78 m)
- polar inertia 51.5 J-s²
- peak rotational speed 12,000 rpm
- peak stored energy 40.7 MJ

As mentioned above, the four-pole configuration allows the use of a metallic through shaft for the CCEML CPA. However, there is still some flux present at the shaft diameter, so a conductive shield is employed to minimize losses. Selection of the shaft diameter and material was a compromise between many factors including:

- machine dynamic performance
- discharge torque material shear and bond shear stresses
- slip ring and brush current densities
- armature conductor slip-ring connections and insulation
- slip ring surface speeds
- bearing permissible speeds
- system weight

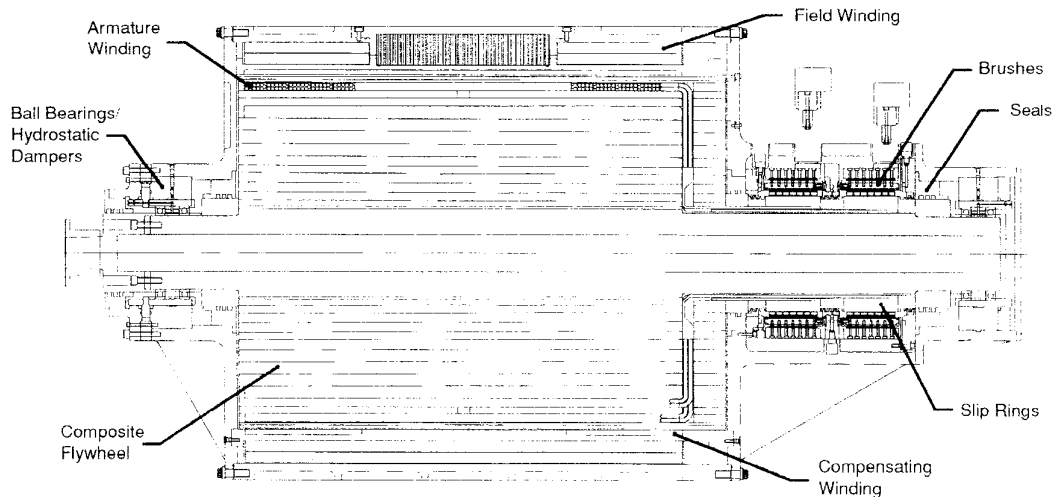


Figure 5. CCEML CPA longitudinal layout (rev 11)

Chosen, was a 6.870 in. (174 mm) diameter Ti6Al4V titanium shaft with bearing journals ground to 5.9055 in. (150 mm) for mounting hybrid angular contact ball bearings with silicon balls. After machining the shaft, the eddy current sleeve is shrunk on followed by a glass reinforced, polyimide resin ring for high temperature resistance between the eddy current shield and subsequent flywheel layers.

The flywheel consists of a series of filament wound IM7 graphite and S2-glass epoxy resin reinforced composite rings press fit together on matching tapers with an interference fit. The amount of interference is a tradeoff between the radial preload required to keep all rings in contact at a 5% design overspeed, and the allowable tensile hoop stresses as determined from internal pressure burst testing. Optimum flywheel radial rigidity and strength is obtained with 100% hoop fibers but allowance must be made for resistance to bending and propagation of cracks. Experience has shown that incorporating 10% axial fibers in hoop wound composites significantly hinders radial crack propagation. In all, eleven rings are pressed together to form the flywheel.

On the surface of the flywheel is mounted the rectangular aluminum litz wire armature-excitation conductor. The ten turn/pole conductor has a cross section of 0.62 in. (15.9 mm) thickness by 1.75 in. (44.5 mm) width and is insulated using a 0.018 in. (0.46 mm) thick braided fiberglass sleeve that will later be vacuum/pressure impregnated with epoxy resin. Following assembly of the armature lap windings, the conductor ends must be attached to the slip rings.

The litz conductor consists of 1,100 individual strands of 22 gage aluminum wire arranged to form 11 bundles of 100 wires. Each of these bundles has a diameter of 0.30 in. (7.6 mm) For four poles, 88 conductor bundles must be routed down the face of the rotor. For space considerations, like polarity wires are paired, brought down the rotor face, and joined to copper crimp joint tabs formed from extensions of concentric copper shaft conductor sleeves. Forty-four of these tabs alternate in polarity around the axis of the machine. The concentric copper sleeves are insulated from the shaft and each other and extend axially out the shaft where copper clad aluminum slip rings are shrunk on.

The final steps in machine assembly are to install a face conductor containment plate, vacuum impregnate the armature/excitation winding, install the armature containment hoop banding, finish grind the bearing surfaces, and perform low speed balancing. Face conductor containment is provided by a nested ring assembly nearly equivalent to the flywheel assembly to provide good growth matching. A glass cloth reinforced epoxy resin ring is then assembled over the flywheel, armature, and end ring assembly, and sealed at the ends to form a closed container for epoxy impregnation of the windings. With that process complete, the glass cloth ring is ground to provide a tapered surface for press fitting the outer banding. Final grinding and low speed balancing are then performed using conventional methods. High speed balancing will be performed in-situ during commissioning of the machine.

Excitation Field Coil and Compensating Winding

The compulsator field coil will be comprised of two concentric aluminum cylinders each divided into four quarter sections that will be spirally cut into a sweet roll configuration and then welded together to form a four pole series winding. Table 3 lists pertinent field coil parameters. A section view of the field coil/compensating winding subassembly is given in figure 6.

Table 3. Field coil parameters

| | |
|----------------------|-------------------------|
| Number of poles | 2 |
| Number of turns/pole | 64 |
| Resistance | 23.28 mΩ |
| Inductance | 2.00 mH |
| Terminal voltage | 3.8 kV |
| Peak current | 25 kA |
| Current Density | 7.64 kA/cm ² |
| Stored Energy | 630 kJ |
| Packing fraction | 87.3 % |
| Weight | 2430 N |

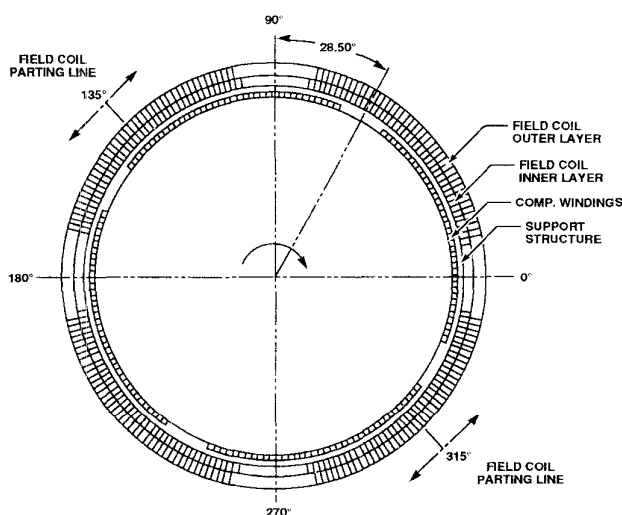


Figure 6. Field coil/compensating windings section (viewed from thrust end)

The concentric cylinders will be forged and final machined from H18 temper 1100 series aluminum billets. A five axis CNC abrasive waterjet system will be employed to cut the sweet roll shapes from the solid cylinders. Each section will then be carefully deburred and thoroughly cleaned and de-oxidized using a sulfuric acid, sodium dichromate, and water solution. Immediately after drying, a 0.13 mm thick coat of Limitrak insulating paint will be electrostatically sprayed over the entire coil section except in the weld zones in order to eliminate re-oxidation of the surfaces, as well as to provide redundant insulation. Each coil section will be spread apart to apply a continuous piece of 0.20 mm thick braided E-glass sleeve with epoxy compatible sizing around each conductor leg. The two halves of the series winding will be constructed utilizing a J-groove configuration and the TIG welding process. Adjacent sections of the inner layer will be welded together along the outermost active length conductor. The appropriate outer layers will then be connected to the inner layers along the innermost end turn conductor. The coil halves will then be assembled around the CWSS and the entire structure inserted into the vacuum impregnation mold. A vacuum pressure impregnation (VPI) process will be used to transfer the resin to the evacuated mold in order to minimize void content.

The purpose of the compensating winding (CW) is to shape the discharge pulse to the launcher. Careful positioning of the selective-passive configuration allows for manageable peak currents with high acceleration ratios (peak acceleration/average acceleration) which minimizes compulsator weight [4]. The position of the CW can also impact field coil charging rates which can heavily influence the generator efficiency [5,6]. The compensating winding support structure (CWSS) consists of a machined titanium forging which supports the four-pole, 42 turn/pole hybrid wound copper compensating conductors. The windings consist of both single shorted turns and series connected patterns. Winding loads are transmitted to the CWSS via sheer in the VPI epoxy matrix. The structure has slots machined into it to maximize the available sheer area for load transmission.

Brush Mechanism

Current collection is accomplished via a brush mechanism connecting the primary armature winding of the compulsator to the gun switch modules. The brush mechanism operates at 3.8 kV and 790 kA. High voltage electrical insulation, current distribution, ohmic heating, and large integrated I^2t values presented the greatest design difficulties. Proven technology from previous designs was employed where possible. Figure 7 shows a detail of the brush mechanism end view layout.

Each terminal of the brush mechanism is made up of twelve rows of seven brushes. The brushes operate at a nominal current density of 3.9 kA/cm² and are formed by silver brazing a 0.635 cm x 1.27 cm x 1.91 cm block of Morganite CM1S copper graphite to four laminated strips of CuNi C70600 copper nickel alloy. The high resistivity of the CuNi is exploited to reduce transient current distribution problems due to inductively preferential current paths through the inner rows of brushes at each terminal. The self-compensating straps are reinforced with a mica insulated stainless steel capture plate bolted to the actuator cap with insulated stainless steel screws. Brush actuation and contact force is provided by a

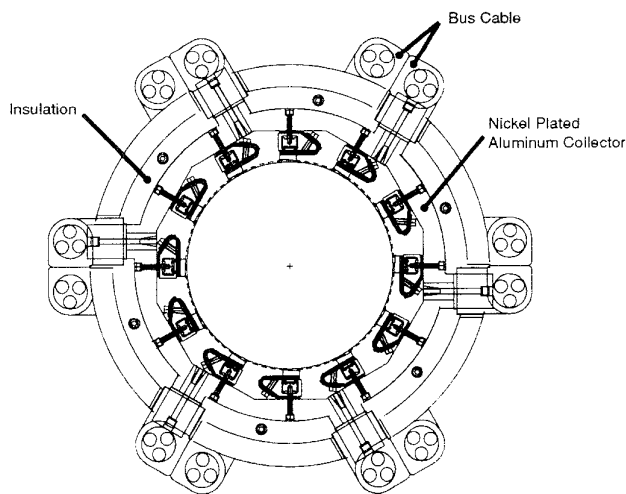


Figure 7. End view of CCEML CPA current collector

Viton bladder molded over a machined 6061 T6 aluminum core, with 100 psi actuation pressure supplied by dry nitrogen gas. Mycalex ceramic inserts are molded into the outer surface of the Viton to act as a thermal barrier between the brush straps and the elastomer. Dry nitrogen gas is also used to provide buffer flow to the center of the labyrinth seal between the two terminals of the brush mechanism, limiting the entrance of brush debris into this region and preventing build up of surface conductivity with the associated tracking breakdown of the insulation system and providing incidental cooling to the brush assemblies. Current from the brush assemblies is transferred through an aluminum collector ring to a set of transposed flexible bus cables. Laminated G-10 evacuation manifolds are located at each end of the brush mechanism to prevent debris build up and contamination of the armature winding and bearing seals.

Power Electronics and Bus

An electrical schematic of the CPA power system is shown in figure 8. The CCEML power supply and integral launch system will feature several innovative designs developed at CEM-UT [7,8]. Whenever possible this system will take advantage of previously

proven pulse power and bus technologies available within the CEM-UT experience base. Specific areas which leverage previous design efforts include the hexapolar flexible buswork, the high density toroidal packaging of parallel solid-state switch elements, capacitor initiation of field coil current during CPA self-excitation, active reclamation of field coil magnetic energy through the use of a full control thyristor based rectifier-inverter bridge, the use of inertial cooling to provide pseudo-steady state operation of all solid state switch elements, and the use of an explosively driven opening switch for circuit protection.

This system will require the use of five distinct switch designs, each with unique operating requirements. Initiation of main gun current will require a repetitive-pulse duty switch with a surge current of 800 kA and a symmetrical voltage rating of 3.8 kV. This switch will be composed of 40 parallel, 77 mm thyristors arranged in a four layer, interleaved, toroidal geometry. Muzzle arc suppression will be require a similar closing switch with identical voltage ratings and a forward surge rating of only 150 kA. Field coil current generation is achieved using a 95 MW thyristor bridge. Each bridge leg will operate at a maximum forward current of 25 kA with a 50% duty and must have a symmetrical voltage stand-off of 3.8 kV. CPA source voltage will be used to drive leg to leg commutation during inverter operation thus achieving effective reclamation of stored field coil energy. Field coil seed current will be provided from a 4 kV capacitive energy store switched by dual 4.5 kV thyristors. Recharging of this store is provided by anti-parallel high voltage diodes with current limiting integral to the diode bus.

Over current and thermal protection of the CPA and all solid state sub-systems is accomplished using an explosively operated opening switch which must carry the combined currents and action demands of both the gun discharge and field coil circuits. During opening this switch must be capable of dissipating all inductive storage energy. Normally, switch initiation is via a standard exploding bridgewire initiator. Fail-safe operation is provided by designing the replaceable switch elements for passive thermal failure beyond normal mission actions. The field winding is also protected by a voltage limiting arc-gap type switch which safely dissipates the stored inductive energy of the field winding should the opening switch be activated while the coil is charged.

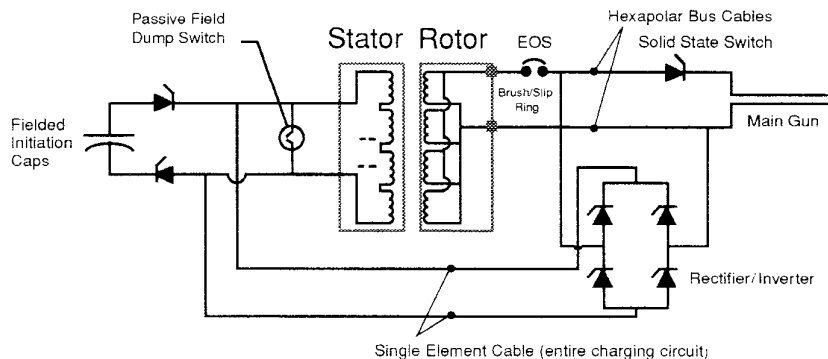


Figure 8. CCEML CPA power circuit schematic

All interconnecting buswork will be designed to allow the use of flexible, hexapolar cable. Both the flex-bus and terminations have been previously built and tested at CEM-UT. Existing flex-bus designs feature "kickless," self-supporting, operation with EM compensation and bipolar terminations. Cable impedances of 108 $\mu\Omega/m$ and 123 nH/m have been demonstrated. Thus, interconnection of the CPA and all switching elements can be completed within the present impedance budget.

Acknowledgments

This program is supported and funded by the United States Marine Corps, and the U.S. Army ARDEC Close Combat Armaments Center under contract number DAAA21-92-C-0060.

References

- [1] W. A. Walls, M. L. Spann, S. B. Pratap, D. A. Bresie, W. G. Brinkman, J. R. Kitzmiller, J. D. Herbst, H. P. Liu, S. M. Manifold, B. M. Rech, "Design of a Self-Excited, Air-Core Compulsator for a Skid-Mounted, Repetitive Fire 9 MJ Railgun System", *IEEE Transactions on Magnetics*, vol. 25, no. 1, Jan 1989.
- [2] J. R. Kitzmiller, R. W. Faidley, R. L. Fuller, R.N. Headifen*, S. B. Pratap, M. L. Spann, R. F. Thelen, "Design of a 600 MW Pulsed Air-Core Compulsator," 1990 International Conference on Electrical Machines.
- [3] J.R. Kitzmiller, R.N. Faidley, R.L. Fuller, R. Headifen, S.B. Pratap, M.L. Spann, R.F. Thelen, "Final Design of an Air Core, Compulsator Driven 60 Caliber Railgun System," *IEEE Transactions on Magnetics*, vol 27, no. 1, January 1991.
- [4] M. D. Driga, S. B. Pratap, and W. F. Weldon, "Design of Compensated Pulsed Alternators with Current Waveform Flexibility," presented at the 6th IEEE Pulsed Power Conference, Arlington, VA, June 29-July 1, 1987.
- [5] S.B. Pratap, "Limitations on the Minimum Charging Time for the Field Coil of Air Core Compensated Pulsed alternators," *IEEE Transactions on Magnetics*, vol 27, no. 1, January 1991.
- [6] S.B. Pratap, K.T. Hsieh, M.D. Driga, and W.F. Weldon, "Advanced Compulsators for Railguns," *IEEE Transactions on Magnetics*, Vol. 25, No. 1, January 1989, pp 454-459.
- [7] R. L. Sledge, D. E. Perkins, and B. M. Rech, "High Power Switches at the Center for Electromechanics at the University of Texas at Austin," *IEEE Transactions on Magnetics*, vol 25, No. 1, January 1989, pp 519-525.
- [8] W. A. Walls et. al. "A Field Based, Self-Excited Compulsator Power Supply for a 9 MJ Railgun Demonstrator," *IEEE Transactions on Magnetics*, vol 27, no. 1, January 1991, pg 335-341.

OPTIMIZATION AND DESIGN OF THE AIR CORE COMPULSATOR FOR THE CANNON CALIBER ELECTROMAGNETIC LAUNCHER SYSTEM (CCEML)

S.B. Pratap, J.R. Kitzmiller, T.A. Aanstoos, K.G. Cook, R.N. Headifen,
R.A. Kuenast, R.A. Lee, H-P Liu, and D.J. Wehrlein

Center for Electromechanics
The University of Texas at Austin
BRC, Mail Code 77000
Austin, TX 78712

Abstract

The Center for Electromechanics at The University of Texas at Austin (CEM-UT) is currently in the manufacturing phase of a skid mounted, compulsator driven 30 mm (round-bore equivalent), rapid fire railgun system. The objective of the 30-month program is to develop a compact, lightweight test bed capable of launching three, five-round salvos of 185-g payloads to 1.85 km/s at a firing rate of 5 Hz. Per contractual requirement, the system is also fully compatible with the Amphibious Assault Vehicle (AAV). This paper describes the results of the optimization process used in determining the power supply requirements for the CCEML. The paper presents the performance specifications and design of the compulsator and critical power electronics resulting from the optimization process. The compulsator (CPA) is a four-pole, self-excited, air-core design which stores the energy for all three salvos inertially.

Introduction

The team of (prime contractor) FMC-NSD and (sub-contractors) CEM-UT and KAMAN Sciences Corporation (KSC) are currently in the design phase of a 30 month effort to design, build, and test an electromagnetic (EM) launcher technology demonstrator with program goals as summarized in table 1. A unique aspect of the program requirements was that desired subprojectile performance at the target was specified; no specifics relative to EM power supplies or system configurations were given. Determining the optimum system configuration required an intensive tradeoff study which looked at nearly all facets of the current EM state-of-the-art including battery-inductor pulsed forming networks (PFN), flywheel-alternator-capacitor PFNs, homopolar generator-inductor PFNs and compulsator PFNs. The results of the tradeoff analysis showed a four-pole, self-excited, field regenerative, selective passive air-core compulsator (CPA) design to be the best choice to satisfy contractual requirements.

Following the tradeoff analysis, the four-pole CPA design was optimized around five independent parameters including launch package mass, muzzle velocity, pulse width, number of shots stored inertially in the rotor, and number of salvos stored inertially in the rotor. In all, over 400 cases were analyzed, each producing a specific optimum CPA design. The overall system optimum configuration settled on launching 15, 185 g launch packages (95 g sub projectile mass) in three, five-shot salvos with a muzzle velocity of 1850 m/s. The shot rate is 300 cpm with a 2.5 s dwell between salvos.

The first part of this paper describes the CPA optimization process and results, as well as predicted performance of the

Table 1. CCEML SOW requirements

| | |
|---|---|
| Armor Penetration (0° and (56° obliquity] | 73 mm (131mm) RHA @ 1,500 m 37 mm (66mm) RHA @ 3,000 m |
| Caliber | 20 -40 mm |
| Firing Rate | 300 - 400 rnds per minute |
| Salvo Size | 5 to 7 rounds (3 salvos total) |
| Time Between Salvos | 2-2.5 s |
| Probability of Hit | 0.9 |
| System Weight | 5,000 lb maximum |
| Weapon Mounting Platform | compatible with AAV |

compulsator. In the second part, the CPA mechanical design is presented, including operating characteristics, general specifications, and design and operation of the power electronics.

CPA Performance and Optimization

The unique aspect of the specifications in this system was that instead of constraining the muzzle energy in the launch package, the penetration at the target at 1.5 and 3.0 km was constrained. This allowed the team to look at some broader, system wide tradeoffs since the launch package mass and the velocity at the muzzle were flexible parameters. Referring back to table 1, the system optimization considered specific issues such as dispersion at the muzzle and the probability of hit in order to determine the optimal shots per salvo and salvos per mission.

In the optimization process the starting point was the design of the penetrator rod (sub-projectile) which was performed by KSC. This was a logical starting point since each sub-projectile was required to meet the penetration requirements at the target. Three different penetrator nose tip radii were considered for five muzzle velocities. The velocity ranged from 1.7 km/s to 2.3 km/s in increments of 150 m/s. For each velocity/nose tip, a projectile was designed with the appropriate aeroballistic and penetration characteristics. Three pulse widths (1.4, 1.7, and 2.0 ms) with the same acceleration ratio (0.5) were considered, implying three peak accelerations which were considered. It was determined that the mid-drive penetrator was not significantly different for the three peak acceleration designs. However the mid-riding tandem solid armature was affected by the peak acceleration issues. This resulted in a total of 45 different launch package designs with corresponding muzzle kinetic energy requirements.

For each of these launch packages an optimized launcher was designed. In this case, optimum was defined as a barrel/launch package combination that resulted in a minimum breech energy requirement. Several interesting tradeoffs were developed as the result of the study.

Augmented vs. Simple Railgun

As indicated earlier the uniqueness of this system was that target penetration requirements rather than muzzle energy was specified. This truly presented an opportunity to minimize the muzzle energy. In any EM launcher the useful energy is that which is imparted to the subprojectile. All other energy including the kinetic energy in the armature represents a loss. An augmented gun typically has extra losses associated with the augmenting turn, with the result that if the muzzle energy of the launch package was fixed it would indicate a higher breech energy requirement. However, with an augmented gun the action ($\int i^2 dt$) through the armature is lower with the result that the armature can be lighter thus resulting in lower muzzle energy requirements. It is therefore conceivable that the breech energy requirements in the augmented gun be lower than a simple gun. Indeed, this was our observation on the CCEML system which finally led to the selection of the augmented gun.

Energy Storage

The pulsed power and energy storage system selected for the CCEML was the compulsator. The size and weight of the pulsed power supply was driven to a large extent by the manner in which energy was apportioned between the prime power and the pulsed power. Considering that the time between salvos is only 0.2 s for a 300 cpm firing rate it is evident that enough kinetic energy needs to be stored in the rotor to complete one salvo. The time between salvos is 2 to 2.5 s. Recharging between salvos requires lower power than recharging between shots but is still considerably high, requiring a turbine which is less traceable to the AAV. However, to conduct an effective tradeoff study machines were designed to store one, two, and three salvos with five, six, and seven shots per salvo, i.e. a total of nine machines for each barrel/launch package combination. The total number of machines thus designed was $45 \times 9 = 405$. Figure 1 summarizes the results of the optimization process. The machine mass was most sensitive to the energy stored in the rotor. Typically it showed a lower mass increment for higher energy storage. This is because given a pulse width, the rotational speed is fixed. Higher energy storage is obtained with larger machine radii and therefore higher energy densities. Over the range of parameters considered the sensitivity of the machine mass to projectile velocity, pulse width and nose tip radius was not significant. For a given energy storage the various machines fell within a 100-g window.

Probability of hit analyses performed by FMC-NSD required a total of three salvos and five shots per salvo at 300 rpm. Considering integration issues it was decided that the machine store enough energy to complete all 15 shots without re-motoring.

Pulse Shape

Three pulse shapes were considered (fig. 2). The common feature in these pulse shapes is that each one has the same peak

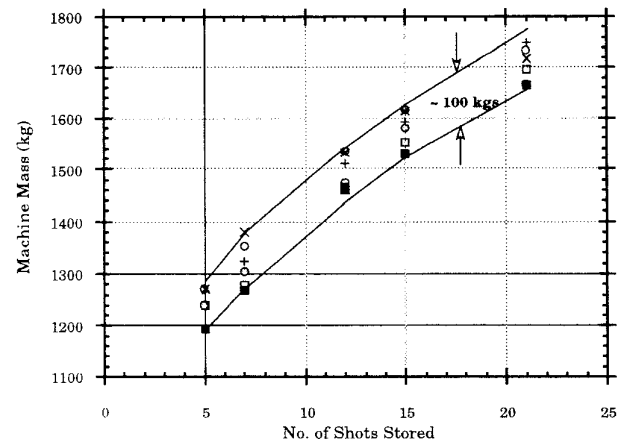


Figure 1. Summary of machines investigated

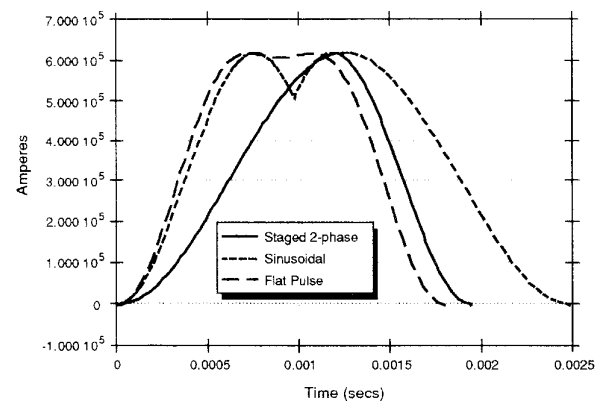


Figure 2. Comparison of various pulse shapes

current and each have the same action. These pulse shapes were obtained with the passive, selective passive, and the staged discharge machines. The acceleration ratio with the passive machine is about 0.38 and the other machines have a ratio of between 0.5 and 0.6. The staged discharge machine is at present an unproved concept and to minimize risk on this project was not pursued. Of the other two pulse shapes, the selective passive machine has a better acceleration ratio and also has a shorter pulse width. This indicates that the machine can spin faster and has a higher energy density. Thus there is a correlation between the pulse shape and the energy density which resulted in the selection of the selective passive machine.

Number of Poles

To get the longest pulse width at the highest tip speed, and therefore highest energy density, it was necessary to keep the number of poles to a minimum. This was especially true of the single phase variant of the compulsator. When energy limited systems are being considered energy density needs to be maximized which normally results in the selection of a two pole machine. However there are some difficulties with a two-pole design. The shaft of the rotor would have to spin through a high magnetic field with a two-pole design. Using a conductive shaft material causes

severe eddy currents. This results in two options, neither of which are desirable. One is to use a ceramic shaft and the other is to use a copper clad metallic shaft. In the latter option the copper which acts as a shield would have to be actively cooled.

The force distribution in a two pole machine is quite non-uniform during discharge. The center of force on the two-pole windings is at diametrically opposite points. This results in higher stresses. The non-uniformity of pressure results in local bending which adds to the hoop stress in the rotor. Also, it is difficult to manage the deflections under the non-uniform loading especially when the clearances between stationary and rotating parts need to be at a minimum.

With the four-pole machine, the field strength reduces at distances away from the field winding towards the center, until at the center the field strength is zero. This permits the use of a conductive shaft which suffers much lower eddy current losses. Also the four-pole winding has the center of force distributed at four equidistant points along the circumference. This load distribution is much easier to manage. Considering these and other advantages the four-pole geometry was selected.

Performance of the System

In a typical operating mode the machine will be driven by a slip clutched, frequency controlled 400 hp (peak) induction motor to a top speed of 12,000 rpm. The torque speed curve will be actively controlled to enable the machine to optimally negotiate the first critical speed. After reaching the top speed the discharge sequence will commence. A typical shot has three distinct events. In the first 100 ms the field coil is charged in a self excitation mode. To initiate this process a capacitor is first discharged into the field coil which provides the seed current. At full field, main gun discharge takes place over 2 ms. Over the next 90 ms part of the magnetic energy stored in the field coil is recovered and returned to the rotor. Throughout the field charging process the motor drives the rotor. During the main discharge when the torque exceeds 400 ft-lb the clutch connecting the motor to the rotor of the compulsator slips thus isolating the motor from the high decelerating torque. After the discharge is complete the motor resynchronizes with the rotor in about 15 ms. In this manner energy is being delivered to the rotor at a slow rate throughout the mission.

The peak current in the gun ranges from 790 kA for the first shot to 650 kA in the last shot. The launch package muzzle energy remains the same for all shots. Figure 3 shows the 15 current pulses during a full engagement. Figure 4 shows variation in the machine speed over the engagement. A little over 50% of the energy is used during a full engagement. The majority of the shots take place without a muzzle arc. However since the machine does slow down to about 70% of its original speed over a full engagement, the last few shots need a muzzle switch to suppress the muzzle arc and ensure that the projectile has minimal dispersion at exit.

CPA Design

CPA Topography and Specifications

As outlined above, the CPA is a four-pole, air-core, selective-passive design which is self-excited and regenerates field energy

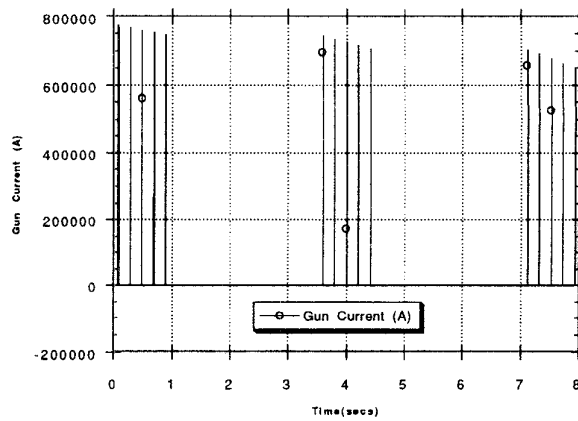


Figure 3. CCEML gun current and machine current during a mission

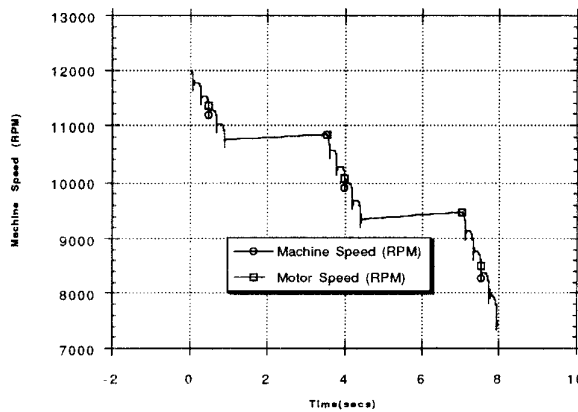


Figure 4. CCEML machine and motor speed during a mission

between each shot. Table 2 lists the CPA pertinent operating specifications. Figure 5 shows the longitudinal cross section of the compulsator. This generation of CPA utilizes a combination of the most attractive features found in previous designs including the Task-C range gun and Small Caliber Compulsator systems [1,2,3]. As discussed above, the four pole design allows for the use of a monolithic through shaft, which is Ti 6Al-4V for the CCEML generator. The CCEML generator features an all titanium stator structure which is made up of four custom castings. The composite rotor is supported on hybrid rolling element bearings which are suspended in full hydrostatic bearing dampers to control dynamic response. Great emphasis was placed on minimizing the CPA weight which makes up for about 70% of the entire system weight.

In the following sections more detail is presented for specific critical components making up the CPA. Also included is a section on the design and operation of the CPA's power electronics.

Rotor

Energy storage for the Cannon Caliber compulsator power supply is provided by a composite flywheel, four pole rotor armature winding, and hoop wound composite banding, all supported on a titanium shaft. The rotor winding serves both excitation and armature duty by means of an external rectifier/inverter discussed

Table 2. CCEML CPA performance parameters

| | | |
|-------------------------------------|--------|-------------------|
| Design Speed | 12,000 | rpm |
| Energy Storage | 40 | MJ |
| Peak Field | 2 | T |
| Peak Open Current Voltage | 3.84 | kV |
| Peak Design Current | 800 | kA |
| Peak Power | 2.4 | GW |
| Discharge Torque | 2.0 | MN-m |
| Electrical Frequency | 400 | Hz |
| Pulse Width | 2 | ms |
| Action (Full Engagement) | 9.15 | GA ^{2-s} |
| Stored Energy Density | 19.3 | J/g |
| Specific Energy Density | 47.6 | MJ/m ³ |
| Power Density | 1160 | W/g |
| Delivered Energy Dens. (Shot) | .29 | J/g |
| Delivered Energy Dens. (Engagement) | 4.35 | J/g |

later in this paper. The rotor assembly has the following specifications:

- diameter 28.66 in. (0.73 m)
- rotor length 39.28 in. (1.00 m)
- overall shaft length 70.78 in. (1.78 m)
- polar inertia 51.5 J-s²
- peak rotational speed 12,000 rpm
- peak stored energy 40.7 MJ

As mentioned above, the four-pole configuration allows the use of a metallic through shaft for the CCEML CPA. However, there is still some flux present at the shaft diameter, so a conductive shield is employed to minimize losses. Selection of the shaft diameter and material was a compromise between many factors including:

- machine dynamic performance
- discharge torque material shear and bond shear stresses
- slip ring and brush current densities
- armature conductor slip-ring connections and insulation
- slip ring surface speeds
- bearing permissible speeds
- system weight

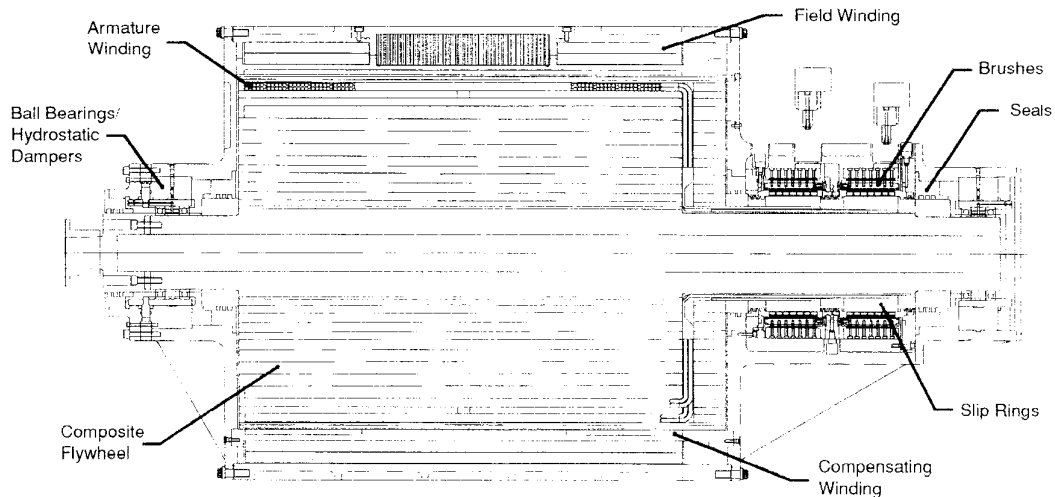


Figure 5. CCEML CPA longitudinal layout (rev 11)

Chosen, was a 6.870 in. (174 mm) diameter Ti6Al4V titanium shaft with bearing journals ground to 5.9055 in. (150 mm) for mounting hybrid angular contact ball bearings with silicon balls. After machining the shaft, the eddy current sleeve is shrunk on followed by a glass reinforced, polyimide resin ring for high temperature resistance between the eddy current shield and subsequent flywheel layers.

The flywheel consists of a series of filament wound IM7 graphite and S2-glass epoxy resin reinforced composite rings press fit together on matching tapers with an interference fit. The amount of interference is a tradeoff between the radial preload required to keep all rings in contact at a 5% design overspeed, and the allowable tensile hoop stresses as determined from internal pressure burst testing. Optimum flywheel radial rigidity and strength is obtained with 100% hoop fibers but allowance must be made for resistance to bending and propagation of cracks. Experience has shown that incorporating 10% axial fibers in hoop wound composites significantly hinders radial crack propagation. In all, eleven rings are pressed together to form the flywheel.

On the surface of the flywheel is mounted the rectangular aluminum litz wire armature-excitation conductor. The ten turn/pole conductor has a cross section of 0.62 in. (15.9 mm) thickness by 1.75 in. (44.5 mm) width and is insulated using a 0.018 in. (0.46 mm) thick braided fiberglass sleeve that will later be vacuum/pressure impregnated with epoxy resin. Following assembly of the armature lap windings, the conductor ends must be attached to the slip rings.

The litz conductor consists of 1,100 individual strands of 22 gage aluminum wire arranged to form 11 bundles of 100 wires. Each of these bundles has a diameter of 0.30 in. (7.6 mm) For four poles, 88 conductor bundles must be routed down the face of the rotor. For space considerations, like polarity wires are paired, brought down the rotor face, and joined to copper crimp joint tabs formed from extensions of concentric copper shaft conductor sleeves. Forty-four of these tabs alternate in polarity around the axis of the machine. The concentric copper sleeves are insulated from the shaft and each other and extend axially out the shaft where copper clad aluminum slip rings are shrunk on.

The final steps in machine assembly are to install a face conductor containment plate, vacuum impregnate the armature/excitation winding, install the armature containment hoop banding, finish grind the bearing surfaces, and perform low speed balancing. Face conductor containment is provided by a nested ring assembly nearly equivalent to the flywheel assembly to provide good growth matching. A glass cloth reinforced epoxy resin ring is then assembled over the flywheel, armature, and end ring assembly, and sealed at the ends to form a closed container for epoxy impregnation of the windings. With that process complete, the glass cloth ring is ground to provide a tapered surface for press fitting the outer banding. Final grinding and low speed balancing are then performed using conventional methods. High speed balancing will be performed in-situ during commissioning of the machine.

Excitation Field Coil and Compensating Winding

The compulsator field coil will be comprised of two concentric aluminum cylinders each divided into four quarter sections that will be spirally cut into a sweet roll configuration and then welded together to form a four pole series winding. Table 3 lists pertinent field coil parameters. A section view of the field coil/compensating winding subassembly is given in figure 6.

Table 3. Field coil parameters

| | |
|----------------------|-------------------------|
| Number of poles | 2 |
| Number of turns/pole | 64 |
| Resistance | 23.28 mΩ |
| Inductance | 2.00 mH |
| Terminal voltage | 3.8 kV |
| Peak current | 25 kA |
| Current Density | 7.64 kA/cm ² |
| Stored Energy | 630 kJ |
| Packing fraction | 87.3 % |
| Weight | 2430 N |

The concentric cylinders will be forged and final machined from H18 temper 1100 series aluminum billets. A five axis CNC abrasive waterjet system will be employed to cut the sweet roll shapes from the solid cylinders. Each section will then be carefully deburred and thoroughly cleaned and de-oxidized using a sulfuric acid, sodium dichromate, and water solution. Immediately after drying, a 0.13 mm thick coat of Limitrak insulating paint will be electrostatically sprayed over the entire coil section except in the weld zones in order to eliminate re-oxidation of the surfaces, as well as to provide redundant insulation. Each coil section will be spread apart to apply a continuous piece of 0.20 mm thick braided E-glass sleeve with epoxy compatible sizing around each conductor leg. The two halves of the series winding will be constructed utilizing a J-groove configuration and the TIG welding process. Adjacent sections of the inner layer will be welded together along the outermost active length conductor. The appropriate outer layers will then be connected to the inner layers along the innermost end turn conductor. The coil halves will then be assembled around the CWSS and the entire structure inserted into the vacuum impregnation mold. A vacuum pressure impregnation (VPI) process will be used to transfer the resin to the evacuated mold in order to minimize void content.

The purpose of the compensating winding (CW) is to shape the discharge pulse to the launcher. Careful positioning of the selective-passive configuration allows for manageable peak currents with high acceleration ratios (peak acceleration/average acceleration) which minimizes compulsator weight [4]. The position of the CW can also impact field coil charging rates which can heavily influence the generator efficiency [5,6]. The compensating winding support structure (CWSS) consists of a machined titanium forging which supports the four-pole, 42 turn/pole hybrid wound copper compensating conductors. The windings consist of both single shorted turns and series connected patterns. Winding loads are transmitted to the CWSS via sheer in the VPI epoxy matrix. The structure has slots machined into it to maximize the available sheer area for load transmission.

Brush Mechanism

Current collection is accomplished via a brush mechanism connecting the primary armature winding of the compulsator to the gun switch modules. The brush mechanism operates at 3.8 kV and 790 kA. High voltage electrical insulation, current distribution, ohmic heating, and large integrated I²t values presented the greatest design difficulties. Proven technology from previous designs was employed where possible. Figure 7 shows a detail of the brush mechanism end view layout.

Each terminal of the brush mechanism is made up of twelve rows of seven brushes. The brushes operate at a nominal current density of 3.9 kA/cm² and are formed by silver brazing a 0.635 cm x 1.27 cm x 1.91 cm block of Morganite CM1S copper graphite to four laminated strips of CuNi C70600 copper nickel alloy. The high resistivity of the CuNi is exploited to reduce transient current distribution problems due to inductively preferential current paths through the inner rows of brushes at each terminal. The self-compensating straps are reinforced with a mica insulated stainless steel capture plate bolted to the actuator cap with insulated stainless steel screws. Brush actuation and contact force is provided by a

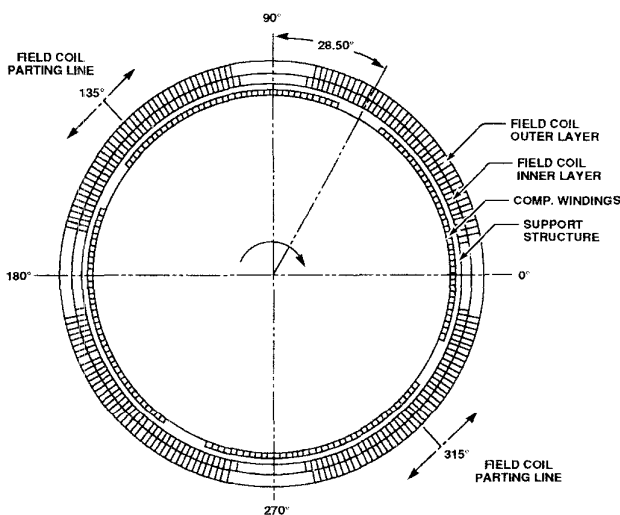


Figure 6. Field coil/compensating windings section (viewed from thrust end)

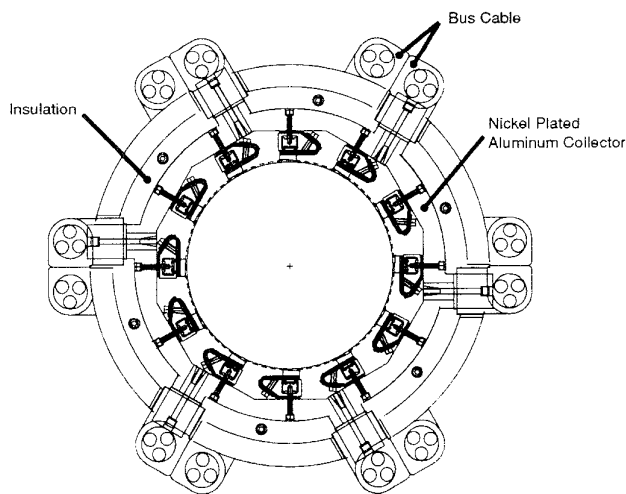


Figure 7. End view of CCEML CPA current collector

Viton bladder molded over a machined 6061 T6 aluminum core, with 100 psi actuation pressure supplied by dry nitrogen gas. Mycalex ceramic inserts are molded into the outer surface of the Viton to act as a thermal barrier between the brush straps and the elastomer. Dry nitrogen gas is also used to provide buffer flow to the center of the labyrinth seal between the two terminals of the brush mechanism, limiting the entrance of brush debris into this region and preventing build up of surface conductivity with the associated tracking breakdown of the insulation system and providing incidental cooling to the brush assemblies. Current from the brush assemblies is transferred through an aluminum collector ring to a set of transposed flexible bus cables. Laminated G-10 evacuation manifolds are located at each end of the brush mechanism to prevent debris build up and contamination of the armature winding and bearing seals.

Power Electronics and Bus

An electrical schematic of the CPA power system is shown in figure 8. The CCEML power supply and integral launch system will feature several innovative designs developed at CEM-UT [7,8]. Whenever possible this system will take advantage of previously

proven pulse power and bus technologies available within the CEM-UT experience base. Specific areas which leverage previous design efforts include the hexapolar flexible buswork, the high density toroidal packaging of parallel solid-state switch elements, capacitor initiation of field coil current during CPA self-excitation, active reclamation of field coil magnetic energy through the use of a full control thyristor based rectifier-inverter bridge, the use of inertial cooling to provide pseudo-steady state operation of all solid state switch elements, and the use of an explosively driven opening switch for circuit protection.

This system will require the use of five distinct switch designs, each with unique operating requirements. Initiation of main gun current will require a repetitive-pulse duty switch with a surge current of 800 kA and a symmetrical voltage rating of 3.8 kV. This switch will be composed of 40 parallel, 77 mm thyristors arranged in a four layer, interleaved, toroidal geometry. Muzzle arc suppression will be require a similar closing switch with identical voltage ratings and a forward surge rating of only 150 kA. Field coil current generation is achieved using a 95 MW thyristor bridge. Each bridge leg will operate at a maximum forward current of 25 kA with a 50% duty and must have a symmetrical voltage stand-off of 3.8 kV. CPA source voltage will be used to drive leg to leg commutation during inverter operation thus achieving effective reclamation of stored field coil energy. Field coil seed current will be provided from a 4 kV capacitive energy store switched by dual 4.5 kV thyristors. Recharging of this store is provided by anti-parallel high voltage diodes with current limiting integral to the diode bus.

Over current and thermal protection of the CPA and all solid state sub-systems is accomplished using an explosively operated opening switch which must carry the combined currents and action demands of both the gun discharge and field coil circuits. During opening this switch must be capable of dissipating all inductive storage energy. Normally, switch initiation is via a standard exploding bridgewire initiator. Fail-safe operation is provided by designing the replaceable switch elements for passive thermal failure beyond normal mission actions. The field winding is also protected by a voltage limiting arc-gap type switch which safely dissipates the stored inductive energy of the field winding should the opening switch be activated while the coil is charged.

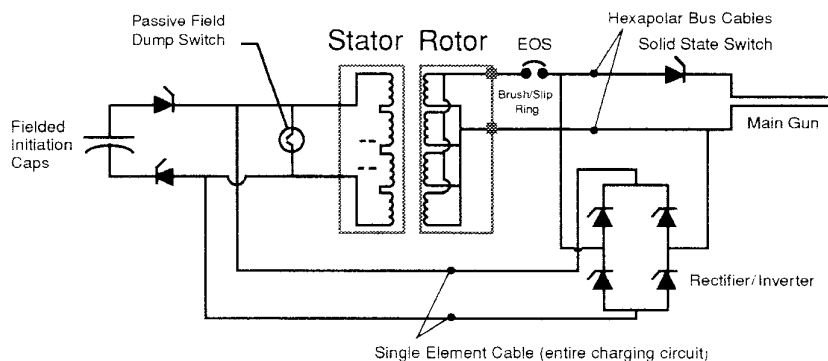


Figure 8. CCEML CPA power circuit schematic

All interconnecting buswork will be designed to allow the use of flexible, hexapolar cable. Both the flex-bus and terminations have been previously built and tested at CEM-UT. Existing flex-bus designs feature "kickless," self-supporting, operation with EM compensation and bipolar terminations. Cable impedances of 108 $\mu\Omega/m$ and 123 nH/m have been demonstrated. Thus, interconnection of the CPA and all switching elements can be completed within the present impedance budget.

Acknowledgments

This program is supported and funded by the United States Marine Corps, and the U.S. Army ARDEC Close Combat Armaments Center under contract number DAAA21-92-C-0060.

References

- [1] W. A. Walls, M. L. Spann, S. B. Pratap, D. A. Bresie, W. G. Brinkman, J. R. Kitzmiller, J. D. Herbst, H. P. Liu, S. M. Manifold, B. M. Rech, "Design of a Self-Excited, Air-Core Compulsator for a Skid-Mounted, Repetitive Fire 9 MJ Railgun System", *IEEE Transactions on Magnetics*, vol. 25, no. 1, Jan 1989.
- [2] J. R. Kitzmiller, R. W. Faidley, R. L. Fuller, R.N. Headifen*, S. B. Pratap, M. L. Spann, R. F. Thelen, "Design of a 600 MW Pulsed Air-Core Compulsator," 1990 International Conference on Electrical Machines.
- [3] J.R. Kitzmiller, R.N. Faidley, R.L. Fuller, R. Headifen, S.B. Pratap, M.L. Spann, R.F. Thelen, "Final Design of an Air Core, Compulsator Driven 60 Caliber Railgun System," *IEEE Transactions on Magnetics*, vol 27, no. 1, January 1991.
- [4] M. D. Driga, S. B. Pratap, and W. F. Weldon, "Design of Compensated Pulsed Alternators with Current Waveform Flexibility," presented at the 6th IEEE Pulsed Power Conference, Arlington, VA, June 29-July 1, 1987.
- [5] S.B. Pratap, "Limitations on the Minimum Charging Time for the Field Coil of Air Core Compensated Pulsed alternators," *IEEE Transactions on Magnetics*, vol 27, no. 1, January 1991.
- [6] S.B. Pratap, K.T. Hsieh, M.D. Driga, and W.F. Weldon, "Advanced Compulsators for Railguns," *IEEE Transactions on Magnetics*, Vol. 25, No. 1, January 1989, pp 454-459.
- [7] R. L. Sledge, D. E. Perkins, and B. M. Rech, "High Power Switches at the Center for Electromechanics at the University of Texas at Austin," *IEEE Transactions on Magnetics*, vol 25, No. 1, January 1989, pp 519-525.
- [8] W. A. Walls et. al. "A Field Based, Self-Excited Compulsator Power Supply for a 9 MJ Railgun Demonstrator," *IEEE Transactions on Magnetics*, vol 27, no. 1, January 1991, pg 335-341.